



**Suzuki–Miyaura Catalyst-Transfer Polycondensation of
Triolborate-Type Fluorene Monomer: Toward Rapid Access
to Polyfluorene-Containing Block and Graft Copolymers from
Various Macroinitiators**

Journal:	<i>Polymer Chemistry</i>
Manuscript ID	PY-ART-08-2020-001127.R1
Article Type:	Paper
Date Submitted by the Author:	01-Oct-2020
Complete List of Authors:	Kobayashi, Saburo; Hokkaido University Fujiwara, Kaiyu; Hokkaido University Jiang, Dai-Hua; Institute of Organic and Polymeric Materials, National Taipei University of Technology Yamamoto, Takuya; Hokkaido University, Division of Applied Chemistry, Faculty of Engineering Tajima, Kenji; Hokkaido University, Faculty of Engineering Yamamoto, Yasunori; Hokkaido University, Division of Chemical Process Engineering Isono, Takuya; Hokkaido University, Faculty of Engineering Satoh, Toshifumi; Hokkaido University, Division of Applied Chemistry, Faculty of Engineering



Suzuki–Miyaura Catalyst-Transfer Polycondensation of Triolborate-Type Fluorene Monomer: Toward Rapid Access to Polyfluorene-Containing Block and Graft Copolymers from Various Macroinitiators

Saburo Kobayashi,^a Kaiyu Fujiwara,^a Dai-Hua Jiang,^{a, b, c} Takuya Yamamoto,^d Kenji Tajima,^d Yasunori Yamamoto,^d Takuya Isono^{*d} and Toshifumi Satoh^{*d}

Received 00th January 20xx,
Accepted 00th January 20xx

DOI: 10.1039/x0xx00000x

www.rsc.org/

In this study, we demonstrated that the Suzuki–Miyaura catalyst transfer polycondensation (SCTP) of the triolborate-type fluorene monomer, viz. potassium 2-(7-bromo-9,9-dihexyl-9H-fluorene-2-yl)triolborate, can be an efficient and versatile approach to the precise synthesis of poly[2,7-(9,9-dihexylfluorene)]s (PFs) and PF-containing block and graft copolymers. SCTP of the triolborate-type monomer proceeded rapidly in a THF/H₂O mixed solvent at –10 °C using an iodobenzene derivative/Pd₂(dba)₃•CHCl₃/t-Bu₃P initiating system. Kinetic and post-polymerization experiments revealed that SCTP proceeded via the chain-growth and living polymerization mechanisms. The most important feature of the present polymerization system is that only a small amount of base and water can sufficiently promote the reaction. The well-controlled nature of this polymerization system enabled the synthesis of high-molecular-weight PFs ($M_n = 5\text{--}69 \text{ kg mol}^{-1}$) with narrow dispersity ($\bar{D}_M = 1.14\text{--}1.38$) and α -end-functionalized PFs. Most importantly, PF-containing block and graft copolymers were successfully synthesized, beginning with various iodobenzene-functionalized macroinitiators; this was difficult to achieve by the conventional SCTP of pinacolboronate-type fluorene monomer. One of the key factors for the successful block and graft copolymer syntheses is the reduced water content in the polymerization medium, which suppressed the potential precipitation/aggregation of the macroinitiators.

Introduction

Poly[2,7-(9,9-dialkylfluorene)]s (PFs) have attracted considerable research attention due to their applications in various organic electronic devices, such as sensors, organic light-emitting diodes (OLEDs),^{1–4} organic field-effect transistors (OFETs),^{5,6} organic photovoltaics (OPVs),^{7–9} and organic memory devices,^{10–13} because of their high fluorescence quantum yield, high thermal stability, high hole mobility, and good solubility in common organic solvents.^{14,15} Many PFs have been synthesized via step-growth polycondensation based on various cross-coupling reactions (e.g., Suzuki–Miyaura coupling and Kumada–Corriu coupling).^{16–18} However, gaining control over the molecular weight and dispersity (\bar{D}_M) of the thus-

synthesized polymers had been difficult owing to the step-growth nature of the polymerization. In 2007, Yokozawa's group reported the Suzuki–Miyaura catalyst transfer polycondensation (SCTP) of an AB-type monomer using PhPd(*t*-Bu₃P)Br as the initiator, in which narrowly dispersed PFs were obtained with a controlled molecular weight.^{19,20} Thus, the SCTP was found to be advantageous over the conventional step-growth polycondensation in terms of both polymerization and structural controls. However, the reported SCTP methods require complicated reaction systems, consisting of a monomer, an initiator (e.g., iodobenzene or bromobenzene derivative), a catalyst (e.g., Pd₂(dba)₃), a ligand like *t*-Bu₃P, a solvent like THF, water, a base like K₃PO₄, and a phase-transfer catalyst like crown ether.^{21–27} Therefore further expansion of the synthetic utility of SCTP is difficult.

For example, synthesis of PF-containing block copolymers (BCPs) have never been achieved using the macroinitiator method, which might be partly attributed to the insufficient initiation efficiency and limited solubility of the macroinitiator in aqueous media. Previously, the PF-containing BCPs had been synthesized either by the coupling reaction of end-functionalized PF with other polymers or by chain extension from end-functionalized PF as the macroinitiator.

^a Graduate School of Chemical Sciences and Engineering, Hokkaido University, Sapporo 060-8628, Japan

^b Institute of Organic and Polymeric Materials, Research and Development Center of Smart Textile Technology, National Taipei University of Technology, 10608 Taipei, Taiwan

^c Institute of Polymer Science and Engineering, National Taiwan University, 106 Taipei, Taiwan

^d Faculty of Engineering and Graduate School of Chemical Sciences and Engineering, Hokkaido University, Sapporo 060-8628, Japan

*E-mail: isono.t@eng.hokudai.ac.jp; satoh@eng.hokudai.ac.jp

Electronic Supplementary Information (ESI) available: Experimental procedures and additional data (¹H NMR, DOSY NMR, SEC, and MALDI-TOF MS). See DOI: 10.1039/x0xx00000x

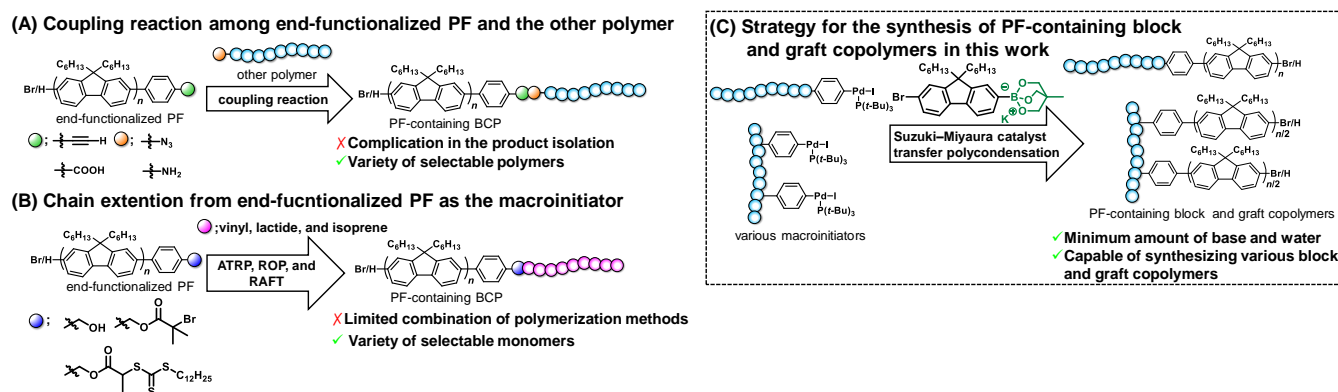


Figure 1. Schematic for the synthesis of the PF-containing block and graft copolymers. (A) Coupling reaction between end-functionalized PF and the other polymer. (B) Chain extension from end-functionalized PF as the macroinitiator. (C) Macroinitiator approach: Our strategy for the synthesis of PF-containing block and graft copolymers by SCTP of triolborate-type fluorene monomer.

In the former approach, it is necessary to add one of the components in excess to complete the reaction, which makes product isolation difficult (Figures 1A).^{28–36} In contrast, the latter approach can avoid such complicated product isolation, making it more synthetically useful (Figures 1B). Nevertheless, the method using PF as the macroinitiator is limited to the combination with atom transfer radical polymerization (ATRP),^{37–39} anionic ring-opening polymerization (ROP),⁴⁰ and reversible addition fragmentation chain transfer (RAFT) polymerization.⁴¹ Since PF-containing block and graft copolymers are promising for a wide variety of device applications,^{4, 6, 10, 12, 13, 28–42} it is of great interest to realize the synthesis of block and graft copolymers via PF chain extension using various macroinitiators.

Therefore, establishing a simpler SCTP system for fluorene monomers is essential for the successful synthesis of PF-containing block and graft copolymers. In this study, we have focused on the use of triolborate salt-type fluorene monomer, instead of the conventional pinacolboronate-type one. In 2008, Miyaura and Yamamoto developed a triolborate salt soluble in organic solvents and stable in air and water, which could be used in Suzuki–Miyaura coupling, even without using water and base. Triolborate salts can be easily synthesized using boronic acid or a boronic acid ester.^{43, 44} In addition, the triolborate salts reportedly show higher reactivity to heteroaromatic compounds and alkyl compounds, which are usually inactive to Suzuki–Miyaura coupling.^{45–47} Therefore, we envisioned that the SCTP of triolborate salt monomers could be performed using a simpler reaction system and eventually offer a drastic improvement in PF synthesis (Figure 1C). Notably, Yokozawa's group investigated the SCTP of a triolborate-type thiophene monomer.⁴⁸ However, the use of a triolborate-type fluorene monomer for SCTP has not yet been investigated.

Herein we investigated the SCTP of a triolborate salt fluorene monomer, viz. potassium 2-(7-bromo-9,9-dialkyl-9H-fluorene-2-yl)triolborate (**M1**), for the first time, aiming to establish a novel precise synthesis strategy for PFs. The living polymerization of the triolborate salt monomer proceeded in a chain-growth manner. Using optimized polymerization conditions, PFs with controlled molecular weights (4,800–

69,400 g mol⁻¹) and a relatively narrow \mathcal{D}_M (1.14–1.38) were successfully synthesized. A variety of α -end-functionalized PFs were then synthesized by SCTP using various functional initiators. Most importantly, we efficiently synthesized PF-containing BCP as well as graft copolymers by SCTP using various macroinitiators, a task that has not been accomplished using conventional SCTP.

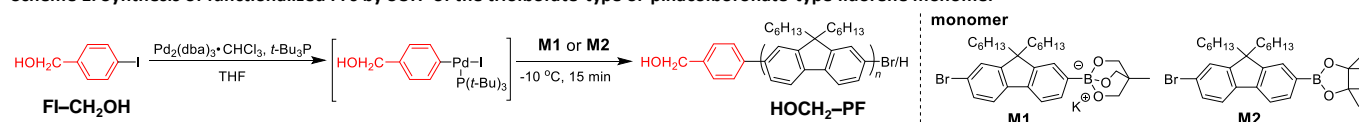
Results and discussion

SCTP of triolborate salt monomer

We first attempted the polymerization of **M1** using the 4-iodobenzyl alcohol (**FI-CH₂OH**) / Pd₂(dba)₃•CHCl₃/t-Bu₃P initiating system at a [**M1**]₀/[**FI-CH₂OH**]₀/[Pd₂(dba)₃•CHCl₃]/[t-Bu₃P] ratio of 15:1:0.3:2.2 at 20 °C in a THF/water (10:1; v/v) solvent system ([**M1**]₀ = 10 mmol L⁻¹, Scheme 1; run 1 in Table 1). Although the SCTP of **M1** occurred, the obtained polymeric product ($M_{n,SEC}$ = 8,500 g mol⁻¹) has a relatively broad \mathcal{D}_M of 1.36. Nevertheless, encouraged by this promising result, we attempted to optimize the reaction conditions. To investigate the effect of the polymerization temperature, SCTP was carried out at -30, -10, and 0 °C, without changing the other factors. At -30 °C (run 4), the product was precipitated out during polymerization. On the other hand, the products obtained at 0 and -10 °C (runs 2 and 3, respectively, in Table 1) exhibited narrower \mathcal{D}_M values of 1.33 and 1.18, respectively. This suggests that possible side reactions, such as chain transfer, were suppressed upon lowering the polymerization temperature.

The chemical structure of the obtained PF was characterized in detail by ¹H NMR spectroscopy and matrix-assisted laser desorption/ionization time-of-flight mass spectroscopy (MALDI-TOF MS). In the ¹H NMR spectrum of the product obtained from run 5 (Figure 2A), the major signals observed were attributed to the polyfluorene backbone (7.93–7.57 ppm: proton A) and the hexyl side chain (2.12 ppm: proton B, 1.36–0.66 ppm: protons C and D), consistent with reported ¹H NMR data.⁴⁰ In addition, a minor signal attributed to the benzyl proton located at the α -chain end (proton E) was observed at 4.79 ppm, suggesting successful incorporation of the initiator residue.

Scheme 1. Synthesis of functionalized PFs by SCTP of the triolborate-type or pinacolboronate-type fluorene monomer

Table 1. SCTP of **M1** under various conditions ^a

run	[monomer] ₀ /[FI-CH ₂ OH] ₀	temp (°C)	<i>M</i> _{n,SEC} ^b (g mol ⁻¹)	<i>M</i> _{n,NMR} ^c (g mol ⁻¹)	<i>D</i> _M ^b	yield ^d (%)
1	15/1	20	8,500	9,500	1.36	80.3
2	15/1	0	8,300	9,200	1.33	85.2
3	15/1	-10	5,700	5,800	1.18	84.3
4	15/1	-30	—	—	—	—
5 ^e	15/1	-10	4,800	4,900	1.14	84.2
6 ^e	30/1	-10	12,300	12,600	1.24	83.2
7 ^e	45/1	-10	14,200	17,800	1.25	84.3
8 ^e	90/1	-10	25,700	29,400	1.28	85.4
9 ^e	180/1	-10	44,700	68,300	1.37	82.6
10 ^e	270/1	-10	69,400	83,300	1.38	88.9
11	270/1	-10	53,100	69,500	1.52	62.0
12 ^f	180/1	-10	24,000	26,700	1.48	86.9

^aPolymerization conditions: Ar atmosphere; solvent, THF/water (10:1, v/v); [**M1**]₀ = 10 mmol L⁻¹; [FI-CH₂OH]₀/[Pd₂(dba)₃•CHCl₃]/[t-Bu₃P] = 1:0.3:2.2.

^bDetermined by SEC (PSt standards, THF, 40 °C). ^cDetermined from ¹H NMR spectrum in CDCl₃. ^dIsolated yields. ^eK₃PO₄ (1.5 equiv.) was added during polymerization. ^f**M2** (180 equiv.), K₃PO₄ (2 mol L⁻¹ aqueous, 150 equiv.), 18-crown-6 (50 equiv.).

Therefore, the obtained product could be the expected PF with a benzyl alcohol residue at the α-chain end (**HOCH₂-PF**). The number-average molecular weight (*M*_{n,NMR}) of the **HOCH₂-PF** (run 5), calculated by end group analysis on the ¹H NMR spectrum, was 4,900 g mol⁻¹. To further confirm the end group fidelity, MALDI-TOF MS analysis was conducted on the obtained **HOCH₂-PF** (run 5). The MALDI-TOF MS spectrum showed a series of peaks at a regular interval of 333.46 Da, corresponding to the 9,9-dihexylfluorene repeating unit (**Figure 2B**). The observed peaks were assigned to the expected chemical structure of **HOCH₂-PF** with a benzyl alcohol moiety at the α-chain end and a hydrogen atom at the ω-end because the peak at *m/z* of 2101.57 matched well with the calculated mass for the hexamer of **HOCH₂-PF** ([M + H]⁺ = 2101.56 Da). Overall, the SCTP of **M1** was found to proceed in a well-controlled manner to produce narrowly dispersed PFs with sufficient end group fidelity.

Living nature of the SCTP of the triolborate salt monomer

The living nature of the SCTP of **M1** was assessed by a kinetic study and post-polymerization experiments. The time-conversion plot for the SCTP of **M1** under the optimized condition revealed that monomer conversion (conv.) reached >99% in 10 min (**Figure 3A**). In addition, the *M*_{n,NMR} of the obtained **HOCH₂-PF** increased linearly with increasing monomer conversion, while the *D*_{MS} were maintained at less than 1.3 over the course of polymerization (**Figure 3B**). These results strongly suggested a chain-growth nature of the polymerization. The kinetic plot revealed distinct first-order kinetic behavior, based on which the rate constant was estimated to be 0.42 s⁻¹ mol L⁻¹ (**Figure 3C**).

The chain extension experiment was conducted to prove the livingness of the propagating chain end. Under the

optimized conditions, the SCTP was initially conducted at a [**M1**]₀/[FI-CH₂OH]₀ ratio of 15:1 for 12 min to achieve full monomer conversion, affording an intermediate product with *M*_{n,NMR} = 5,760 g mol⁻¹ and *D*_M = 1.28. Then, an additional 15 eq. of **M1** was added to the reacting mixture for the second polymerization step. Importantly, the added monomer was fully consumed, as confirmed by ¹H NMR analysis. The SEC traces of the products obtained after the first and second polymerization steps are shown in **Figure 3D**, which demonstrates the shift in the elution peak maximum toward the higher-molecular-weight region after the second polymerization step. This is strong evidence in favor of the initiation of second polymerization from the living chain end. These results collectively suggest that polymerization of the triolborate salt monomer **M1** proceeded via living polymerization in a chain-growth manner.

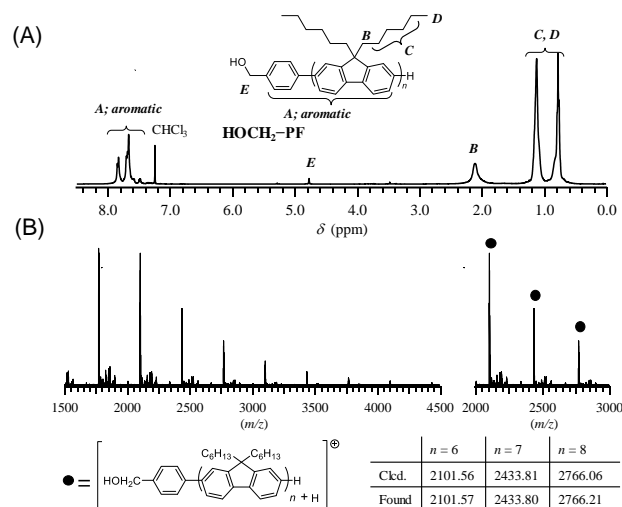


Figure 2. (A) ^1H NMR in CDCl_3 (400 MHz) and (B) MALDI-TOF MS spectra of $\text{HOCH}_2\text{-PF}$ obtained from run 5 (Table 1).

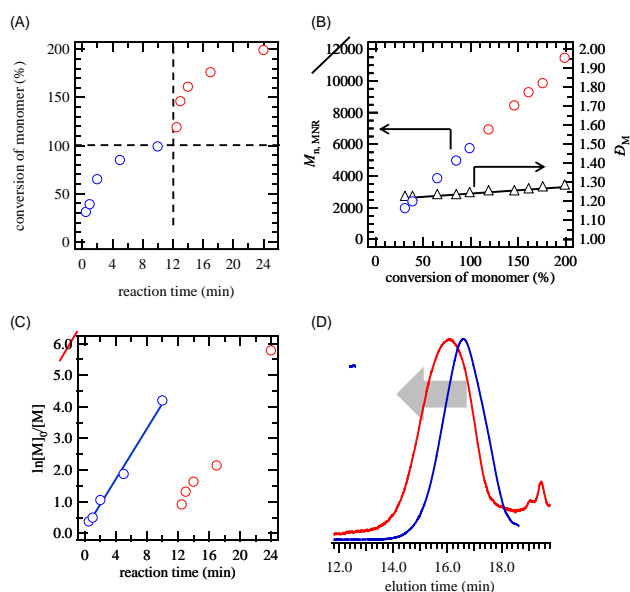


Figure 3. (A) Plot of time against conversion (blue, first polymerization; red, post-polymerization) for SCTP of **M1** at $[\text{M1}]_0/[\text{FI-CH}_2\text{OH}]_0/[\text{Pd}_2(\text{dba})_3\cdot\text{CHCl}_3]/[\text{t-Bu}_3\text{P}]$ ratio of 15:1:0.3:2.2 in THF/water (10:1, v/v) at -10°C . (B) Dependence of $M_{n,\text{NMR}}$ (blue, first polymerization; red, post-polymerization) and \mathcal{D}_M (triangle, dispersity) on monomer conversion. (C) First-order kinetic plots for SCTP (blue, first polymerization; red, post-polymerization). (D) SEC traces of PFs obtained before (blue line) and after (red line) second polymerization (eluent, THF; flow rate, 1.0 mL min^{-1}).

Control of molecular weight

With the above-mentioned promising results in hand, we tried to optimize the polymerization condition to produce high-molecular-weight PFs with narrow \mathcal{D}_M . After thorough investigation, the addition of a small amount of a base (K_3PO_4) was found to be effective in improving the \mathcal{D}_M (run 5, $M_{n,\text{SEC}} = 4,800\text{ g mol}^{-1}$ (THF), $\mathcal{D}_M = 1.14$), due to the anion-ligand exchange of the Pd complex upon addition of the base, which further facilitated the catalysis.⁴⁹

With the optimized polymerization condition in hand, the SCTPs of **M1** were conducted by varying the $[\text{M1}]_0/[\text{FI-CH}_2\text{OH}]_0$ ratio (30:1 for run 6, 45:1 for run 7, 90:1 for run 8, 180:1 for run 9, and 270:1 for run 10) to synthesize high-molecular-weight PFs. As a result, PFs with $M_{n,\text{SEC}} = 10,000\text{--}69,400\text{ g mol}^{-1}$ and $\mathcal{D}_M = 1.24\text{--}1.38$ (runs 6–10, Table 1, $M_{n,\text{NMR}} = 12,600\text{--}83,300\text{ g mol}^{-1}$) were successfully obtained (Figure 4). It is notable that the highest molecular weight achieved by the present polymerization system was higher than that achieved thus far by the SCTP of the pinacolboronate-type fluorene monomer.²⁵ On the other hand, SCTP of **M1** at the $[\text{M1}]_0/[\text{FI-CH}_2\text{OH}]_0$ ratio of 270/1 without K_3PO_4 (run 11 in Table 1) gave a PF with much lower $M_{n,\text{SEC}}$ of $53,100\text{ g mol}^{-1}$ and much higher \mathcal{D}_M of 1.52 compared to the one obtained in the presence of K_3PO_4 . For comparison, we examined the polymerization of 2-(7-bromo-9,9-dihexyl-9H-fluorene-2-yl)4,4,5,5-tetramethyl-1,2,3-dioxaborolane (**M2**), the conventional pinacolboronate-type

fluorene monomer, with the $\text{FI-CH}_2\text{OH}/\text{Pd}_2(\text{dba})_3\cdot\text{CHCl}_3/\text{t-Bu}_3\text{P}/\text{K}_3\text{PO}_4/18\text{-crown-6}$ initiating system for a $[\text{M2}]_0/[\text{FI-CH}_2\text{OH}]_0$ ratio of 180:1 at -10°C in THF/ H_2O (10:1, v/v).⁴⁰ However, the obtained $\text{HOCH}_2\text{-PF}$ had much lower $M_{n,\text{SEC}}$ ($24,000\text{ g mol}^{-1}$) and broader \mathcal{D}_M (1.48) than those obtained in run 12, possibly due to chain transfer to the monomer. These results demonstrate that the triolborate salt monomer is better suited for the synthesis of higher-molecular-weight PFs.

Synthesis of α -chain-end-functionalized PFs using functional initiators

To make the polymerization technique described herein more useful and versatile as a general synthetic tool for PFs, it is important to achieve further functionalization by end functionalization.

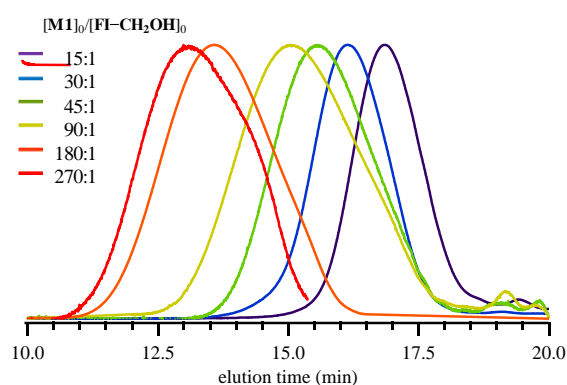


Figure 4. SEC traces of PFs obtained using different $[\text{M1}]_0/[\text{FI-CH}_2\text{OH}]_0$ ratios (purple line, 15:1; blue line, 30:1; green line, 45:1; yellow line, 90:1; orange line, 180:1; red line, 270:1) detected by RI detector (eluent, THF; flow rate, 1.0 mL min^{-1}).

Scheme 2. Synthesis of α -end-functionalized PFs via SCTP using functional initiators

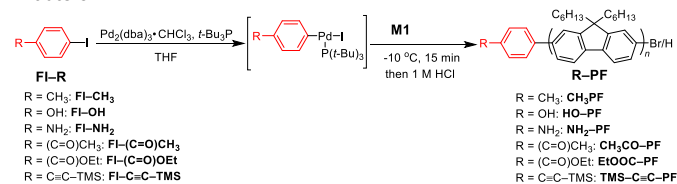


Table 2. Synthesis of α -end-functionalized PFs via SCTP using various initiators^a

run	α -end group	$M_{n,\text{SEC}}^b$ (g mol^{-1})	$M_{n,\text{NMR}}^c$ (g mol^{-1})	\mathcal{D}_M^b	yield ^d (%)
13	$-\text{CH}_3$	4,800	4,400	1.35	86.8
14	$-\text{OH}$	5,100	5,300	1.27	85.8
15	$-\text{NH}_2$	5,000	5,100	1.19	73.0
16	$-(\text{C}=\text{O})\text{CH}_3$	5,300	5,700	1.36	83.3
17	$-(\text{C}=\text{O})\text{OEt}$	5,200	4,100	1.23	81.7
18	$-\text{C}\equiv\text{C-TMS}$	6,000	7,700	1.35	82.8

^aTHF/water (v/v) = 10:1; $[\text{M1}]_0 = 10\text{ mmol L}^{-1}$; $[\text{M1}]_0/[\text{FI-R}]_0/[\text{Pd}_2(\text{dba})_3\cdot\text{CHCl}_3]/[\text{t-Bu}_3\text{P}]/[\text{K}_3\text{PO}_4] = 15:1:0.3:2.2:1.5$.

^bDetermined by SEC (PSt standards, THF, 40°C). ^cDetermined by ^1H NMR spectroscopy in CDCl_3 . ^dIsolated yields.

Thus, we first performed the SCTP of **M1** using a variety of functional iodobenzene derivatives (**FI-CH₃**, **FI-OH**, **FI-NH₂**, **FI-(C=O)CH₃**, **FI-(C=O)OEt**, and **FI-C≡C-TMS**) as the initiator under the optimized reaction conditions ($[\text{FI-R}]_0/[\text{M1}]_0$ ratio = 1:15, in THF/H₂O (10:1, v/v), at -10 °C), producing α -end-functionalized PFs (**Scheme 2**, **Table 2**). All the polymerizations proceeded homogeneously and were quenched by adding 1 mol L⁻¹ HCl. The $M_{n,SEC}$ and D_M of the obtained PFs were 4,400–6,000 g mol⁻¹ and 1.19–1.36, respectively (**Figure S1**). In the ¹H NMR spectrum of the PF obtained using **FI-CH₃** (run 13), a characteristic signal appeared at 2.45 ppm, attributed to the methyl protons of the tolyl group (proton **F**), along with major signals attributed to the PF backbone (**Figure S2**). Similarly, ¹H NMR signals originating from the initiator residues were confirmed, along with those arising from the main chain of PF for the other products; the signal at 3.51 ppm (proton **G**) was attributed to the methyl proton of **-(C=O)CH₃**; the signals at 4.45 ppm (**H**) and 1.45 ppm (**I**) were assigned to the methylene and methyl protons, respectively, of **-(C=O)OEt**; and the signal at 0.08 ppm (**J**) corresponded to the methyl protons of **-C≡C-TMS** (**Figure S2**).

To confirm the end group fidelity, we employed MALDI-TOF MS analysis. For the PF obtained using **FI-CH₃**, the MALDI-TOF MS spectrum exhibited two series of peaks at a regular interval of 333.11 Da (**Figure S3 (a)**). The observed peaks denoted by closed circles were assigned to the expected chemical structure of **CH₃-PF** having a tolyl moiety at the α -chain end and a proton at the ω -chain end, because the peak at 2085.54 Da matched well with the calculated mass for the hexamer of **CH₃-PF** ($[\text{M}+\text{H}]^+ = 2085.54$ Da). Although the peaks due to the **CH₃-PF** with a bromine atom at the ω -chain end were also observed (denoted by open circles), a tolyl group was always incorporated at the α -chain end. In the MALDI-TOF MS spectrum of the PFs obtained using **FI-OH**, **FI-NH₂**, **FI-(C=O)CH₃**, **FI-(C=O)OEt** and **FI-C≡C-TMS** as the initiator, the peak for the corresponding hexamer was observed at 2087.62, 2087.52, 2113.56, 2097.54, and 2168.10, respectively, all of which agreed well with the m/z values calculated for the corresponding hexamer PF with a -OH, -CH₃, -NH₂, -(C=O)CH₃, -(C=O)OEt, and -C≡C-TMS group at the α -chain end (**Figure S3**). The MALDI-TOF MS analysis undoubtedly demonstrated that the obtained PFs were indeed the desired α -chain end tolyl-, phenol-, aniline-, ketone-, ester-, and trimethylsilylethynyl-functionalized PFs (**CH₃-PF**, **HO-PF**, **H₂N-PF**, **CH₃CO-PF**, **EtOOC-PF**, and **TMS-C≡C-PF**, respectively). More importantly, these results demonstrated the good functional group tolerance of the proposed SCTP process.

Synthesis of PF-containing block and graft copolymers using macroinitiator

Given the good functional group tolerance and the well-controlled nature of the polymerization system described herein, a variety of polymers should be applied as the macroinitiator. Such an approach can be effective for the synthesis of PF-containing block and graft copolymers. It should

be noted that the utility of the combination of the macroinitiator approach and catalyst-transfer polycondensation was very recently disclosed in the synthesized polythiophene-containing BCPs.⁵⁰ Thus, we investigated the SCTP of **M1** using various iodobenzene-functionalized macroinitiators to produce PF-containing block and graft copolymers. Notably, the water content in the solvent was reduced as much as possible to avoid possible precipitation of the macroinitiator. As summarized in **Table S2**, the water content in the solvent did not affect the polymerization properties, and we found that the SCTP of **M1** proceeds smoothly even in the THF/water (5000:1, v/v) solvent system. With this information in hand, we attempted the SCTP of **M1** with the iodobenzene-terminated polystyrene (**PSt-I**; $M_{n,NMR} = 2,150$ g mol⁻¹, $D_M = 1.17$, run 19) as the macroinitiator under the optimized polymerization conditions ($[\text{PSt-I}]_0/[\text{M1}]_0 = 1:30$; THF/water (v/v) = 5000:1; **Table 3**), producing **PSt-b-PF** diblock copolymer in one step (**Scheme 3A**). SEC analysis revealed that **M1** polymerization indeed proceeded from **PSt-I**, as evidenced by a clear shift in the elution peak toward the higher-molecular-weight region with virtually no tailing (**Figure 5A**). In addition, the ¹H NMR spectrum of the product showed signals attributed to both the PF and PSt main chain (**Figure S5**), demonstrating the successful formation of **PSt-b-PF**. The $M_{n,NMR}$ for the PF block was determined to be 12,700 g mol⁻¹. To further verify the formation of the BCP, we employed diffusion-order NMR spectroscopy (DOSY). In the DOSY spectrum (**Figure 6**), only a single diffusion coefficient ($D = 2.23$ mm² s⁻¹) was observed for all the ¹H NMR signals due to both the blocks, evidencing the covalent attachment between the PF and PSt blocks. These results clearly demonstrated the success in the PF-containing BCP synthesis using the macroinitiator method.

One of the key factors for the successful BCP synthesis should be the reduced water content in the solvent. To test this hypothesis, we examined the polymerization of **M1** with **PSt-I** in the THF/water (10:1, v/v) solvent system. As expected, the product was a mixture of the diblock copolymer and the unreacted macroinitiator (**Figure S4**). The increased water content in the polymerization medium likely induced precipitation/aggregation of the macroinitiators, as evidenced by the cloudy polymerization mixture. This is in clear contrast to the result obtained by following the SCTP approach described herein: the polymerization system was homogeneous due to good solubility in the solvent with a minimal amount of water. To further verify the advantage of using the triolborate-type monomer, we performed BCP synthesis using **M2** with **PSt-I** in THF/water (10:1 and 5000:1, v/v) (**Table S3**). However, in both cases, SEC analysis of the products revealed the formation of a trace amount of the BCP (**Figure S4**), demonstrating that the combination of the triolborate-type monomer and reduced water content in the solvent is essential for successful BCP synthesis.

Scheme 3. (A) Syntheses of PSt-*b*-PF, PLA-*b*-PF, PCL-*b*-PF, and PEO-*b*-PF by SCTP using PSt-I, PLA-I, PCL-I, and PEO-I, respectively. (B) Syntheses of PF-*b*-PCL-*b*-PF, (PCL-*b*-PF)₃, and PBA-*g*-PF by SCTP using (PCL-I)₂, (PCL-I)₃, and P(BA_{50-co}-Bzl₄), respectively

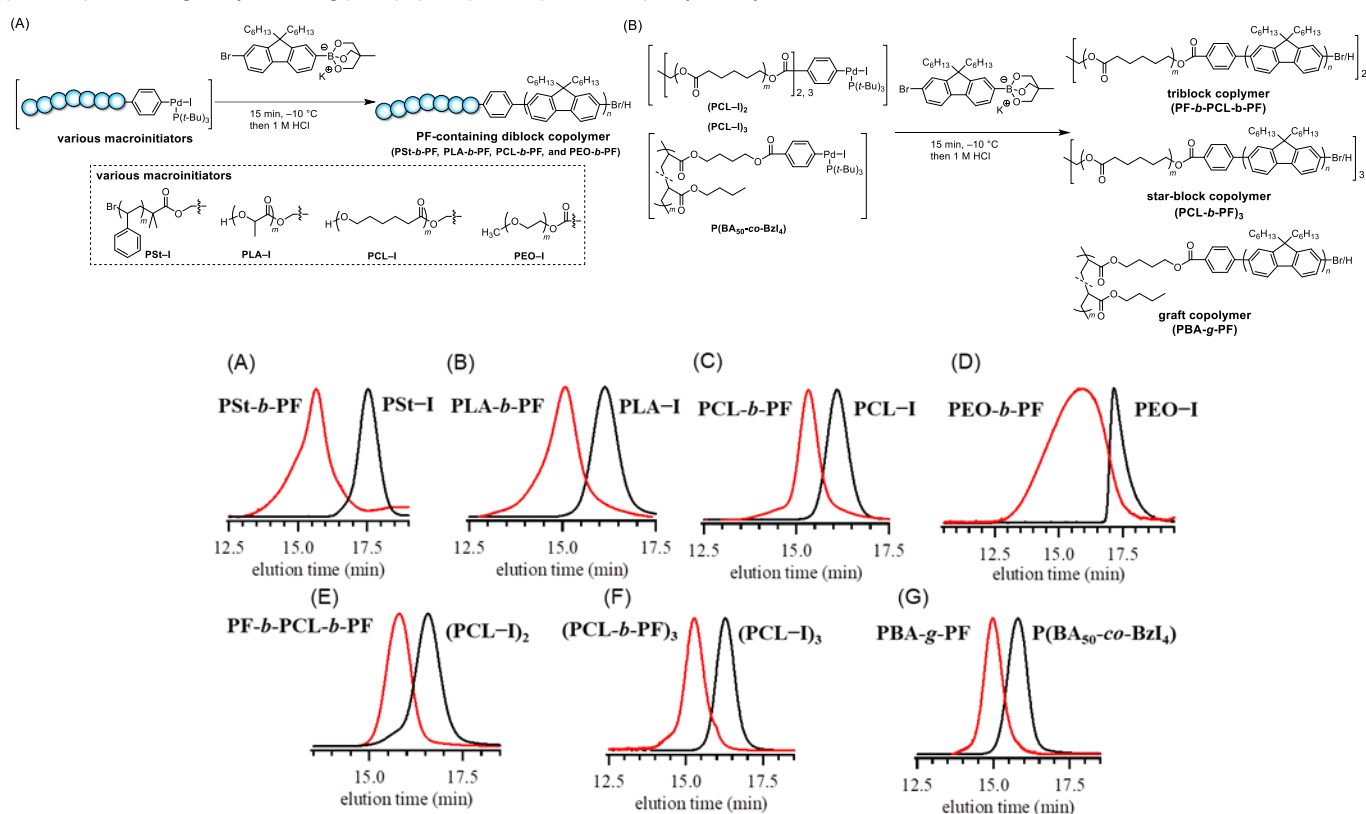


Figure 5. SEC traces of PF-containing block and graft copolymers (red curves: A, PSt-*b*-PF; B, PLA-*b*-PF; C, PCL-*b*-PF; D, PEO-*b*-PF; E, PF-*b*-PCL-*b*-PF; F, (PCL-*b*-PF)₃; and G, PBA-*g*-PF) and the corresponding macroinitiators (black curves: A, PSt-I; B, PLA-I; C, PCL-I; D, PEO-I; E, (PCL-I)₂; F, (PCL-I)₃; and G, P(BA_{50-co}-Bzl₄)) detected by RI detector (eluent, THF; flow rate, 1.0 mL min⁻¹).

Table 3. Polymerization of triolborate-type fluorene monomer using various macroinitiators^a

run	macroinitiator	copolymer		yield ^d (%)		
		$M_{n,NMR}^c$ (g mol ⁻¹)	\mathcal{D}_M^b			
19	PSt-I	2,150	1.17	12,700	1.20	87.0
20	PLA-I	6,000	1.06	15,700	1.19	90.0
21	PCL-I	6,700	1.07	16,000	1.11	85.0
22	PEO-I	5,300	1.25	14,200	1.50	67.3
23 ^e	(PCL-I) ₂	7,900	1.05	17,800	1.10	88.5
24 ^f	(PCL-I) ₃	7,300	1.05	17,100	1.07	82.6
25 ^g	P(BA _{50-co} -Bzl ₄)	8,100	1.09	21,300	1.08	76.3

^aPolymerization conditions: Ar atmosphere; solvent, THF/water (v/v) = 5000:1; [M1]₀ = 10 mmol L⁻¹; [M1]₀/[macroinitiator]₀/[Pd₂(dba)₃•CHCl₃]/[t-Bu₃P]/[K₃PO₄] = 30:1:0.5:2.2:1.5. ^bDetermined by SEC (PSt standards, THF, 40 °C). ^cDetermined by ¹H NMR spectrum in CDCl₃. ^dIsolated yield was calculated based on the mass recovery of the product. ^e[M1]₀/[macroinitiator]₀/[Pd₂(dba)₃•CHCl₃]/[t-Bu₃P]/[K₃PO₄] = 30:1:1.5:4.4:3.0. ^f[M1]₀/[macroinitiator]₀/[Pd₂(dba)₃•CHCl₃]/[t-Bu₃P]/[K₃PO₄] = 30:1:1.5:6.6:4.5. ^g[M1]₀/[macroinitiator]₀/[Pd₂(dba)₃•CHCl₃]/[t-Bu₃P]/[K₃PO₄] = 40:1:2.0:8.8:6.0.

The versatility of the presented BCP synthesis was further demonstrated by conducting SCTP with a variety of iodobenzene-terminated macroinitiators, such as linear poly(*rac*-lactide) (PLA-I; $M_{n,NMR}$ = 6,000 g mol⁻¹, \mathcal{D}_M = 1.06, run 20), poly(ϵ -caprolactone) (PCL-I; $M_{n,NMR}$ = 6,700 g mol⁻¹, \mathcal{D}_M = 1.07, run 21), and poly(ethylene oxide) (PEO-I; $M_{n,NMR}$ = 5,300 g mol⁻¹, \mathcal{D}_M = 1.25, run 22) in THF/water (5000:1, v/v) ([macroinitiator]₀/[M1]₀ = 1:30) (Scheme 3A). Table 3 summarizes the polymerization results. All the polymerizations proceeded homogeneously and gave the corresponding diblock copolymers, i.e., PLA-*b*-PF, PCL-*b*-PF, and PEO-*b*-PF with \mathcal{D}_M values in the range 1.11–1.50, in good yields. Figure 5 shows the SEC traces of the obtained BCPs and the corresponding macroinitiators. The elution peak of the macroinitiator shifted to the higher-molecular-weight region after the SCTP of M1, indicating that the SCTP was initiated from the corresponding macroinitiators. The ¹H NMR spectra of the obtained BCPs exhibited characteristic signals due to the macroinitiator block, as well as those arising from the PF block (Figure S5), which further confirmed the successful BCP synthesis.

To further expand this approach, we examined macroinitiators possessing multiple iodobenzene initiating sites (Scheme 3B).

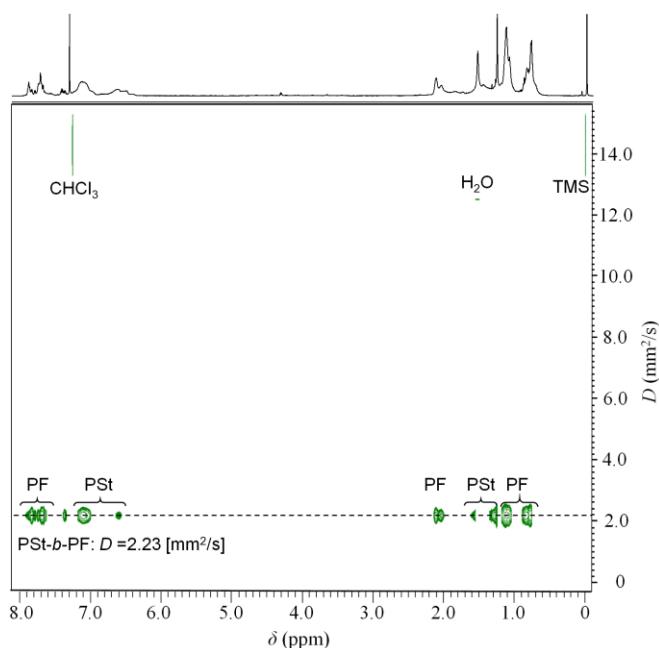


Figure 6. DOSY NMR spectrum of **PSt-*b*-PF** (run 1, Table S3) in CDCl_3 (600 MHz).

Thus, the SCTP of **M1** was conducted using linear $(\text{PCL-I})_2$; $M_{n,\text{NMR}} = 7,900 \text{ g mol}^{-1}$, $\mathcal{D}_M = 1.05$, $[(\text{PCL-I})_2]_0/[\text{M1}]_0 = 1:30$; run 23) and three-armed star-shaped PCLs having an iodobenzene at each chain end $(\text{PCL-I})_3$; $M_{n,\text{NMR}} = 7,300 \text{ g mol}^{-1}$, $\mathcal{D}_M = 1.05$, $[(\text{PCL-I})_3]_0/[\text{M1}]_0 = 1:30$; run 24) as the macroinitiators to produce a **PF-*b*-PCL-*b*-PF** triblock copolymer and $(\text{PCL-*b*-PF})_3$ three-armed star-block copolymers. In addition, poly(*n*-butyl acrylate) having multiple iodobenzene moieties on the side chain $(\text{P}(\text{BA}_{50}\text{-co-Bzl}_4))$; $M_{n,\text{NMR}} = 8,100 \text{ g mol}^{-1}$, $\mathcal{D}_M = 1.09$, $[\text{P}(\text{BA}_{50}\text{-co-Bzl}_4)]_0/[\text{M1}]_0 = 1:40$; run 25) was employed as the macroinitiator to produce a PF-containing graft copolymer **(PBA-*g*-PF)**. The ^1H NMR and SEC analyses confirmed the successful synthesis of the targeted triblock, star-block, and graft copolymers (Figures 5 and S6).

Conclusions

In conclusion, we successfully demonstrated that the SCTP of the triolborate-type fluorene monomer can be an efficient and versatile approach to the precise synthesis of high-molecular-weight end-functionalized PFs with narrow dispersity as well as PF-containing block and graft copolymers. Kinetic and post-polymerization studies revealed that the SCTP proceeded rapidly through the chain growth and living polymerization route. The most important feature of the polymerization system described herein is that only a small amount of base and water can promote the SCTP, unlike the conventional SCTP of the pinacolboronate-type fluorene monomer, which requires large amounts of base and water. In addition, the well-controlled polymerization allowed direct access to PF-containing block and graft copolymers by combining with various macroinitiators by SCTP. One of the key factors for the successful block and graft copolymer syntheses is the reduced water content in the polymerization medium, which suppressed the potential precipitation/aggregation of the macroinitiators. Therefore,

SCTP of the triolborate salt fluorene monomer offers the advantage of achieving precise polymerization in a simpler reaction system and affords well-defined PFs with various functionalities at the chain ends. We believe that the use of triolborate-type monomers in SCTP can lead to significant progress in the fabrication of high-quality π -conjugated polymers with unique structures and functions, which can eventually contribute to the development of organic light-emitting diodes, organic photovoltaics, and organic memory devices.

Conflicts of interest

There are no conflicts to declare.

Acknowledgements

This work was financially supported by the JSPS Grant-in-Aid for Scientific Research (B) (Grant Number: 19H02769), MEXT Grant-in-Aid for Scientific Research on Innovative Areas (Hybrid Catalysis for Enabling Molecular Synthesis on Demand; Grant Numbers: 18H04639 and 20H04798), and JST CREST (Grant Number JPMJCR19T4), Frontier Chemistry Center (Hokkaido University), Photo-excitonix Project (Hokkaido University), and Creative Research Institute (CRIS, Hokkaido University).

Notes and references

- J. H. Burroughes, D. D. C. Bardley, A. R. Brown, R. N. Marks, K. Mackay, R. H. Friend, P. L. Burns, and A. B. Holmes, *Nature*, 1990, **347**, 539–541.
- M.-C. Choi, Y. Kim, and C.-S. Ha, *Prog. Polym. Sci.*, 2008, **33**, 581–630.
- A. C. Grimsdale, K. L. Chan, R. E. Martin, P. G. Jokisz, and A. B. Holmes, *Chem. Rev.*, 2009, **109**, 897–1091.
- D.-H. Jiang, S. Kobayashi, C.-C. Jao, Y. Mato, T. Isono, Y.-H. Fang, C.-C. Lin, T. Satoh, S.-H. Tung, and C.-C. Kuo, *Polymers*, 2020, **12**, 84–95.
- B. S. Ong, Y. Wu, Y. Li, P. Liu, and H. Pan, *Chem. Eur. J.*, 2008, **14**, 4766–4778.
- F. Cicoira, and C. Santato, *Adv. Funct. Mater.*, 2007, **17**, 3421–3434.
- K. M. Coakley, and M. D. McGehee, *Chem. Mater.*, 2004, **16**, 4533–4542.
- S. Gunes, H. Neugebauer, and N. S. Sariciftci, *Chem. Rev.*, 2007, **107**, 1324–11338.
- G. Li, R. Zhu, and Y. Yang, *Photonics*, 2012, **6**, 153–161.
- Q.-D. Ling, D.-J. Liaw, C. Zhu, D. S.-H. Chan, E.-T. Kang, and K.-G. Neoh, *Prog. Polym. Sci.*, 2008, **33**, 917–978.
- B. Cho, S. Song, Y. Ji, T.-W. Kim, and T. Lee, *Adv. Funct. Mater.*, 2011, **21**, 2806–2829.
- Y.-C. Chiu, C.-C. Shih, and W.-C. Chen, *J. Mater. Chem. C.*, 2015, **3**, 551–558.
- J.-C. Hsu, A. Hirao, and W.-C. Chen, *J. Mater. Chem.*, 2012, **22**, 5820–5827.
- D. Neher, *Macromol. Rapid Commun.*, 2001, **22**, 1365–1385.
- U. Scherf, and E. J. W. List, *Adv. Mater.*, 2002, **14**, 477–487.
- T. Yamamoto, *Macromol. Rapid Commun.*, 2002, **23**, 583–606.

- 17 F. Babudri, G. M. Farinola, and F. Naso, *J. Mater. Chem.*, 2004, **14**, 11–34.
- 18 G. Barbarella, M. Melucci, and G. Sotgiu, *Adv. Mater.*, 2005, **17**, 1581–1593.
- 19 A. Yokoyama, H. Suzuki, Y. Kubota, K. Ohuchi, H. Higashimura, and T. Yokozawa, *J. Am. Chem. Soc.*, 2007, **129**, 7236–7237.
- 20 T. Yokozawa, and A. Yokoyama, *Chem. Rev.*, 2009, **109**, 5595–5619.
- 21 K. Kosaka, T. Uchida, K. Mikami, Y. Ohta, and T. Yokozawa, *Macromolecules*, 2018, **51**, 364–369.
- 22 H.-H. Zhang, C.-H. Xing, and Q.-S. Hu, *J. Am. Chem. Soc.*, 2012, **134**, 13156–13159.
- 23 H.-H. Zhang, C.-H. Xing, G. B. Tsemo, and Q.-S. Hu, *ACS Macro Lett.*, 2013, **2**, 10–13.
- 24 H.-H. Zhang, Q.-S. Hu, and K. Hong, *Chem. Commun.*, 2015, **51**, 14869–14872.
- 25 H.-H. Zhang, C.-H. Xing, Q.-S. Hu, and K. Hong, *Macromolecules*, 2015, **48**, 967–978.
- 26 H.-H. Zhang, W. Peng, J. Dong, and Q.-S. Hu, *ACS Macro Lett.*, 2016, **5**, 656–660.
- 27 J. Dong, H. Guo, and Q.-S. Hu, *ACS Macro Lett.*, 2017, **6**, 1301–1304.
- 28 Y. K. Kwon, and M. S. Kim, *Macromolecules*, 2009, **42**, 887–891.
- 29 H. H. Ahn and Y. K. Kwon, *Polymer*, 2013, **54**, 4864–4872.
- 30 P. Chen, G. Yang, T. Liu, T. Li, M. Wang, and W. Huang, *Polym. Int.*, 2006, **55**, 473–490.
- 31 Y.-C. Chiu, C.-C. Kuo, C.-J. Lin, and W.-C. Chen, *Soft Matter*, 2011, **7**, 9350–9358.
- 32 P. Leclere, M. Surin, and R. Lazzaroni, *Eur. Polym. J.*, 2004, **40**, 885–892.
- 33 Y.-C. Chiu, Y. Chen, C.-C. Kuo, S.-H. Tung, T. Kakuchi, and W.-C. Chen, *ACS Appl. Mater. Interfaces*, 2012, **4**, 7, 3387–3395.
- 34 H.-C. Hsieh, C.-C. Hung, K. Watanabe, J.-Y. Chen, Y.-C. Chiu, T. Isono, Y.-C. Chiang, R. R. Reghu, T. Satoh, and W.-C. Chen, *Polym. Chem.*, 2018, **9**, 3820–3831.
- 35 C. S. Fisher, M. C. Baier, and S. Mecking, *J. Am. Chem. Soc.*, 2013, **135**, 1148–1154.
- 36 J.-T. Wang, K. Saito, H.-C. Wu, H.-S. Sun, C.-C. Hung, Y. Chen, T. Isono, T. Kakuchi, T. Satoh and W.-C. Chen, *NPG Asia Materials*, 2016, **8**, 1–11.
- 37 J.-J. Li, J.-J. Wang, Y.-N. Zhou, and Z.-H. Luo, *RSC Adv.*, 2014, **4**, 19869–19877.
- 38 A. Bolonesi, F. Galeotti, U. Giovannella, F. Bertini, and S. Yunus, *Langmuir*, 2009, **25**, 533–5338.
- 39 S. Huber, and S. Mecking, *Macromolecules*, 2019, **52**, 5917–5924.
- 40 K. Saito, T. Isono, H.-S. Sun, T. Kakuchi, W.-C. Chen and T. Satoh, *Polym. Chem.*, 2015, **6**, 6959–6972.
- 41 A.-N. A.-Duong, C.-C. Wu, Y.-T. Li, Y.-S. Huang, H.-Y. Cai, I.J. Hai, Y.-H. Cheng, C.-C. Hu, J.-Y. Lai, C.-C. Kuo, and Y.-C. Chiu, *Macromolecules*, 2020, **53**, 4030–4037.
- 42 H.-S. Sun, Y.-C. Chiu, W.-Y. Lee, Y. Chen, A. Hirao, T. Satoh, T. Kakuchi, and W.-C. Chen, *Macromolecules*, 2015, **48**, 3907–3917.
- 43 (a) *Organic Synthesis via Boranes, Vol. 2* (Eds.: H. C. Brown and M. Zaidlewicz), Aldrich, Milwaukee. 2001; (b) *Science of Synthesis, Hauben-Weyl Methods of Molecular Transformations, Vol. 6* (Eds.: D. E. Kaufmann and D. S. Matteson), Thieme, Stuttgart. 2005; (c) *Boronic Acids* (Ed.: D. G. Hall), Wiley-VCH, Weinheim. 2005.
- 44 (a) N. Miyaura, A. Suzuki, *Chem. Rev.*, 1995, **95**, 2457–2483; (b) N. Miyaura, *Organoboron Compounds. Top. Curr. Chem.*, 2002, **219**, 11–59; (c) *Organic Synthesis via Boranes, Vol. 3* (Eds.: A. Suzuki and H. C. Brown), Aldrich, Milwaukee. 2003; (d) *Metal-Catalyzed Cross-Coupling Reactions*, 2nd ed. (Eds.: A. Meijere and F. Diederich), Wiley-VCH, Weinheim. 2004, 41–123.
- 45 Y. Yamamoto, M. Takizawa, X.-Q. Yu, and N. Miyaura, *Angew. Chem. Int. Ed.*, 2008 **47**, 928–931.
- 46 G.-Q. Li, Y. Yamamoto, and N. Miyaura, *Tetrahedron*, 2011, **67**, 6804–6811.
- 47 S. Sakashita, M. Takizawa, J. Sugai, H. Ito, and Y. Yamamoto, *Org. Lett.*, 2013, **15**, 4308–4311.
- 48 K. Kosaka, Y. Ohta, and T. Yokozawa, *Macromol. Rapid Commun.*, 2015, **36**, 373–377.
- 49 C. Amatore, A. Jutans, and G. L. Duc, *Chem. Eur. J.*, 2011, **17**, 2492–2503.
- 50 H.-N. Choi, H.-S. Yang, J.-H. Chae, T.-L. Choi, and I.-H. Lee, *Macromolecules*, 2020, **53**, 5497–5503.

Graphical Abstract

